Spin Crossover

DOI: 10.1002/anie.201204207

Four-Site Cooperative Spin Crossover in a Mononuclear Fe^{II} Complex**

Anders Lennartson, Andrew D. Bond, Stergios Piligkos, and Christine J. McKenzie**

Spin crossover (SCO), one of the most impressive examples of molecular bistability, is of interest for a number of applications in molecular electronics, including molecular memory, switches, and sensors. SCO-active Fe^{II} compounds switch between high-spin (HS, $^5T_2$) and low-spin (LS, $^1A_1$) electronic states in response to an external stimulus such as temperature, pressure, light irradiation, or magnetic/electric fields. The HS↔LS transition, which is accompanied by a visible color change, can be abrupt, gradual, and/or hysteretic. Dinuclear[1] and polynuclear[2] Fe^{II} compounds showing two-step SCO have been synthesized, based on the hypothesis that SCO sites are most likely to communicate if they are covalently linked. In two-step SCO, the HS↔LS transition proceeds via a thermodynamically stable intermediate electronic state, typically comprising a specific stoichiometric combination of HS and LS Fe^{II} atoms. Synthesis of Fe^{II} compounds that can exhibit more than three addressable magnetic states has proven to be more difficult. For example, only three of the five simple integral electronic states that are potentially available through four-site cooperativity (4HS, 3HS:1LS, 2HS:2LS, 1HS:3LS, and 4LS) have been detected magnetically and/or spectroscopically in molecular ferrous squares.[3] Non-integral three-step SCO has been found for a two-dimensional coordination polymer, $[Fe^{II}(4\text{-methylpyridine})_2\{Au(CN)_2\}_2]$,[4] and there have also been serendipitous discoveries of cooperative SCO in mononuclear Fe^{II} complexes.[5] The latter are naturally confined to the crystalline state, and examples to date have been limited to two-step SCO. Most have furnished three addressable magnetic states, comprising all HS, equivalent numbers of HS:LS, and all LS. One reported example, $[Fe^{II}(isoxazole)_6](BF_4)_2$, shows a 3HS, 2HS:1LS, 1HS:2LS combination (with the 3LS state apparently inaccessible), on account of three-site cooperativity derived from trigonal symmetry in the crystal structure.[5e] Crystal polymorphism has been shown to influence the magnetic properties of Fe^{II} SCO complexes,[6] illustrating explicitly the importance of the crystalline arrangement for realizing multi-step cooperative behavior.

We have synthesized a new mononuclear Fe^{II} SCO complex, $[(bpte)Fe^{II}(NCSe)_2]$ (bpte = *S*,*S*′-bis(2-pyridylmethyl)-1,2-thioethane,[7] $NCSe^-$ = isoselenocyanate; Scheme 1). This compound is unusual in the context of SCO in that it contains two S donor atoms, while the vast majority of SCO systems reported to date are based on N_6 donor ligands. The compound exhibits a remarkable solid-state chemistry: we have isolated and characterized four polymorphic crystalline phases, which we label α, β, γ, and δ in order of their chronological discovery. We find that one phase is SCO-inactive (β), one exhibits one-step SCO (γ), and two exhibit four-site cooperative SCO (α and δ). The four-site cooperativity is unprecedented, and it is remarkable that it is observed for a mononuclear Fe^{II} compound.

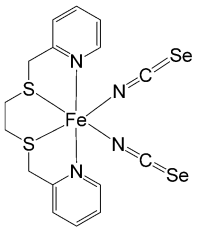

Scheme 1. Chemical formula of $[(bpte)Fe^{II}(NCSe)_2]$.

$[(bpte)Fe^{II}(NCSe)_2]$ was isolated as a yellow to green crystalline material from the 1:1:2 reaction of bpte, $[Fe^{II}(OTf)_2(MeCN)_2]$, and potassium selenocyanate in water/acetonitrile mixtures under an inert N_2 atmosphere. Once isolated, the crystals could be handled in air and exhibit long-term stability. A variation in crystal color within the chemically homogenous sample gave the first hint of the existence of multiple electronic states. Different crystal morphologies were also evident. Selection of the various colors and morphologies (Figure 1) eventually led to crystallographic characterization of the four polymorphs. Bulk samples of the α and δ phases sufficient for magnetic susceptibility measurements could be obtained by hand selection of the various single crystals, aided by the fact that these crystals were typically large (millimeter dimensions) and distinct in their morphologies. Manual separation was more difficult for the β and γ phases, which are much smaller. For the γ phase, a bulk sample for magnetic measurements was obtained, although it was contaminated to some degree by the β phase (see below). For the β phase, it was possible only to measure single-crystal X-ray diffraction data on the few crystals that we could isolate. The crystallographic results show that the β phase is not SCO active in the examined temperature range of 300–100 K.

[*] Dr. A. Lennartson, Prof. A. D. Bond, Prof. C. J. McKenzie
Department of Physics, Chemistry and Pharmacy
University of Southern Denmark
Campusvej 55, 5230 Odense (Denmark)
E-mail: adb@chem.sdu.dk
mckenzie@sdu.dk
Dr. S. Piligkos
Department of Chemistry
University of Copenhagen
Universitetsparken 5, 2100 Copenhagen (Denmark)

[**] We thank the Danish Council for Independent Research/Natural Sciences for financial support (grant no. 272-08-0436) to C.J.M. and for a Sapere Aude fellowship (10-081659) to S.P. The sequential variable-temperature diffraction data were collected at the application laboratory of Agilent Technologies, Abingdon, U.K., with the hospitality and assistance of Dr. Marcus Winter and Dr. Alex Griffin.

Supporting information for this article is available on the WWW under http://dx.doi.org/10.1002/anie.201204207.

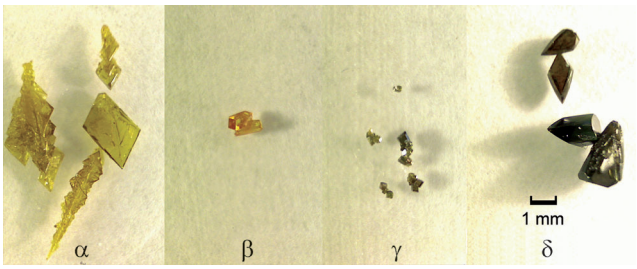

Figure 1. Crystals of the four polymorphic phases isolated for [(bpte)$Fe^{II}(NCSe)_2$] at room temperature.

Variable-temperature magnetic-susceptibility measurements for the α, γ, and δ phases over the range 370–2 K (Figure 2) show $\chi_m T \approx 3.4$–$3.6\ cm^3 mol^{-1} K$ at the upper temperature limit, typical for HS Fe^{II} atoms. Upon cooling, the

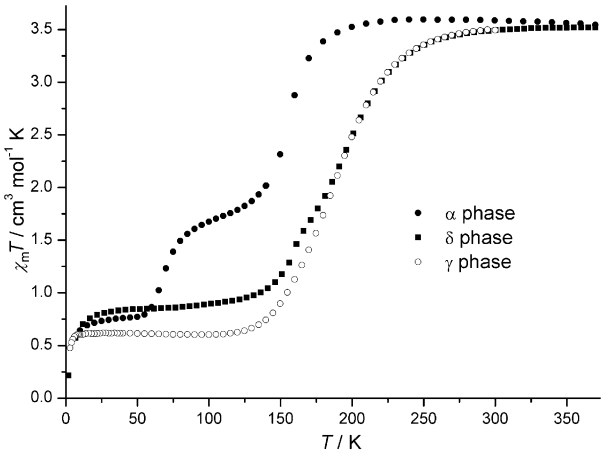

Figure 2. Variable-temperature magnetic susceptibility measurements for the α, γ, and δ phases.

γ phase shows a one-step transition to reach a plateau of $0.62\ cm^3 mol^{-1} K$ at approximately 120 K. This indicates the presence of a paramagnetic impurity, most likely some of the β phase. The β phase is established by crystallographic measurements to remain HS down to at least 100 K. The residual $\chi_m T$ value of the γ phase below 120 K corresponds to around 16 % of β phase contamination (on average, one hand-picked crystal out of every six). Even though a d_6 LS Fe^{II} atom is never fully diamagnetic (because of spin-orbit coupling mediated mixing of the $^1A_1$ ground state to the paramagnetic excited states), we attribute this residual paramagnetism to β phase contamination because of its sizeable magnitude. Upon reheating of the γ phase, there is no thermal hysteresis.

Upon cooling the α phase, $\chi_m T$ decreases quite abruptly at approximately 175 K, traversing a plateau-like region with only a minor decline over the temperature range 140–80 K. The value of $\chi_m T \approx 1.8\ cm^3 mol^{-1} K$ for this plateau corresponds to a 1:1 ratio of HS:LS Fe^{II} sites. From approximately 80 K, a second abrupt decrease is observed down to a second plateau having $\chi_m T \approx 0.8\ cm^3 mol^{-1} K$, which then persists down to around 20 K. The $\chi_m T$ value for this second plateau is appropriate for a 1HS:3LS state. Below approximately 20 K, the curve drops towards zero because of complete conversion to the LS state and/or zero field-splitting effects of the HS state. Upon reheating the α phase, thermal hysteresis is observed in the temperature range 50–80 K (see Supporting Information, Figure S1).

Upon cooling the δ phase, the $\chi_m T$ versus T curve displays a much more gradual decline down to around 130 K, at which point a plateau emerges that is stable to around 20 K. Again, this plateau appears at $\chi_m T \approx 0.8\ cm^3 mol^{-1} K$, appropriate for a 1HS:3LS Fe^{II} state. A minor shoulder in the region 150–175 K suggests a 1HS:1LS state, but clearly this has only a very limited temperature range of stability. Neither the α nor the δ phases exhibit any indication of a plateau for the 3HS:1LS state ($\chi_m T \approx 2.5\ cm^3 mol^{-1} K$). Upon reheating, the δ phase displays no thermal hysteresis.

For the one-step SCO γ phase, the crystal structure in the range 300–100 K contains two molecules in the crystallographic asymmetric unit (see Supporting Information). Upon cooling, the Fe–S bond distances in both molecules change simultaneously from an average value of 2.551(1) Å at 300 K to 2.240(1) Å at 100 K without any crystallographically distinguishable intermediate state. The Fe–N bond distances mirror these trends. The absolute changes in the Fe–N bond distances are smaller than those for Fe–S (approximately 0.2 Å for Fe–N compared to approximately 0.3 Å for Fe–S, upon changing from HS to LS). The precision of the Fe–S bond distances determined by the X-ray analysis is higher than that for the Fe–N bond distances (see Supporting Information). This is typical for SCO compounds, which often show Fe^{II} atoms that appear intermediate between HS and LS on account of limited resolution and/or spatial averaging caused by disorder of the HS/LS sites.[8] The changes in the Fe–S bond distances and in the unit-cell volume follow sigmoidal curves that resemble the shape of the magnetic susceptibility curve (see Supporting Information). The magnetic susceptibility measurements suggest an average 1HS:1LS composition around the inflection point at 180 K, and two-component disorder becomes evident for the S-$(CH_2)_2$S linker unit in one of the crystallographically distinct complexes around this temperature. Initially, a new S$(CH_2)_2$S orientation appears as a minor disorder component, and progresses to a 50:50 site occupation as the structure is cooled to 100 K.

For the δ phase at 300 K, the structure can be described in the orthorhombic space group $Pbn2_1$ with a single HS Fe^{II} complex in the asymmetric unit. At 250 K, however, the diffraction data are more consistent with a reduction of symmetry to the monoclinic space group *Pn* (retaining the same unit-cell setting) with two crystallographically distinct Fe^{II} complexes. In some crystals, the S$(CH_2)_2$S units within the two independent molecules appear to be ordered, while in other crystals disorder is observed for one of the complexes in the asymmetric unit. The monoclinic structure remains close to the orthorhombic metric and the crystals commonly appear to be twinned. Further cooling below 250 K causes the Fe–S bonds in one of the crystallographically distinct complexes to contract in a sigmoidal fashion, while the other complex remains essentially unchanged in the HS state (see Supporting Information), showing only a gradual contraction from

around 200 K. At 155 K, an abrupt doubling of the crystallographic *b* axis is observed (Supporting Information, Movie S4). The space group remains *Pn*, thereby giving four Fe^{II} complexes in the crystallographic asymmetric unit. In the structure at 155 K, two of the crystallographically distinct complexes are clearly in the LS state (average Fe–S = 2.249(5) and 2.247(4) Å), one is clearly in the HS state (average Fe–S = 2.548(5) Å), while the fourth appears to be somewhere between (average Fe–S = 2.315(5) Å). Further cooling causes the Fe–S bonds of the latter complex to contract, reaching an ordered 1HS:3LS state at around 130 K, consistent with the plateau at $\chi_m T \approx 0.8\ cm^3 mol^{-1} K$ in the magnetic susceptibility data. This ordered 1HS:3LS structure was obtained repeatedly for several crystals from different batches, and shows conclusively the four-site cooperative nature of the system.

Comparing the crystal structures of the four polymorphs, it is clear that the lack of SCO activity for the β phase is accompanied by a significantly different molecular structure (Figure 3). In particular, the thioselenate ligands adopt Fe–C–N angles of approximately 150°, compared to an angle

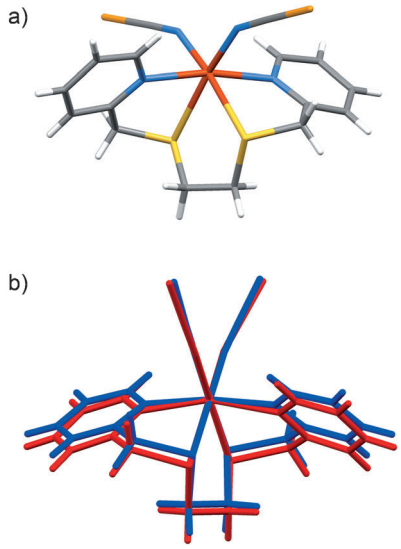

Figure 3. a) Molecular structure of the non-SCO-active β phase. C, gray, H white, Fe red, S yellow, N blue. b) Representative molecular structure for the SCO-active α, γ, and δ phases, showing the change in conformation during the HS(red)→LS(blue) transition. See also Supporting Information, Movie S3.

much closer to linear in the three SCO-active polymorphs. The molecular conformation in the α, γ, and δ phases is closely comparable, and the change in conformation that accompanies the HS→LS transitions is also similar in all three cases (see Figure 3 and Supporting Information, Movie S3). The local point symmetry of the FeS_2N_4 coordination set approximates C_{2v}, and the coordination angles become closer to a regular orthogonal arrangement in the LS state. In particular, the *cis* S–Fe–S angle changes from around 83° in the HS state to around 90° in the LS state, and the *trans* angle between the N atoms of the pyridyl rings changes from approximately 162° to 173°. The Fe–S bonds also contract to a larger degree than the Fe–N bonds on account of their softer nature. This change in the geometry of the FeS_2N_4 coordination set is accompanied by a substantial change in the conformation of the bpte ligand, with the pyridyl rings and $S(CH_2)_2S$ units moving significantly as a result of the SCO transition. The ordering and disordering phenomena described for the $S(CH_2)_2S$ units in the α, γ, and δ phases must reflect a change in the crystallographic environment around the bpte ligands upon cooling of the crystals, and this is probably a subtle precursor to the correlated SCO transitions.

The crystal structures of the α and δ polymorphs contain comparable two-dimensional sections, that is, they are polytypes (Figure 4). The consistent layers in the structures contain ribbons where the Fe–CNSe arms of the complexes "embrace" the $S(CH_2)_2S$ units of adjacent complexes, with the phenyl rings of the bpte ligands interdigitated between neighboring ribbons. In the centrosymmetric α phase, the layers are stacked so that the ribbons run in opposing directions, while in the non-centrosymmetric δ phase, all ribbons are aligned in the same direction. Although it is tempting to link the comparable cooperative SCO behavior of the α and δ phases directly to their polytypic nature, closer

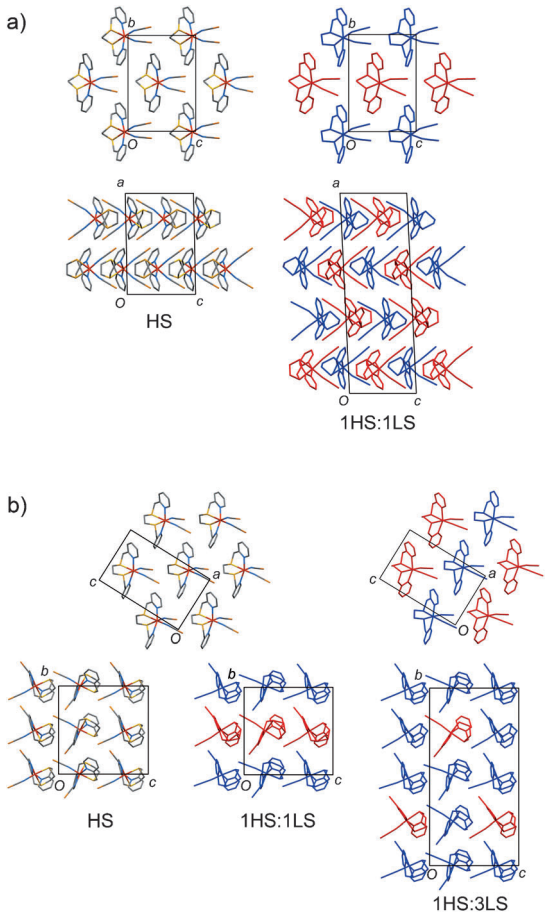

Figure 4. Crystal structures of the α (a) and δ (b) phases, showing the comparable 2D sections and the stacking of those sections. The "ribbons" referred to in the text run horizontally. At 300 K (left), all complexes are in the HS state. At lower temperatures (right), red complexes are in the HS state and blue complexes are in the LS state.

inspection reveals that the cooperative SCO behavior does not occur consistently in the two structures. In the α phase (Figure 4a), the 1HS:1LS state observed at 100 K has HS and LS complexes in alternate ribbons within each layer. In the δ phase, however, the 1HS:1LS state observed at 200 K has complete layers of HS complexes alternating with complete layers of LS complexes. Furthermore, in the 1HS:3LS state at 100 K, the layers with 1HS:1LS stoichiometry have HS and LS complexes alternating along ribbons (Figure 4b), rather than having complete HS and complete LS ribbons as in the α phase. Thus, there could be some relationship between the polytypic nature of α and δ phases and their comparable four-site cooperative SCO behavior, but a concrete description of the intermolecular interactions that mediate the cooperativity is difficult to identify.

Weber et al.[9] demonstrated high cooperativity through an exceptionally wide thermal hysteresis loop in a mononuclear SCO iron(II) compound containing an FeO_2N_4 coordination set. This observation, together with the FeS_2N_4 system presented here, demonstrate that asymmetric donor sets may give rise to new or more extreme SCO properties. In seeking to rationalize the four-site cooperative SCO behavior for $[(bpte)Fe^{II}(NCSe)_2]$, one feature of the bpte ligand that differs from other Fe^{II} SCO complexes studied to date is the presence of the S donor atoms. The asymmetry in the FeS_2N_4 coordination set is exaggerated as the complex undergoes the HS→LS transition on account of the relative softness of the Fe–S bonds compared to the Fe–N bonds. Thus, the SCO process invokes significant conformational change in the polydentate ligand, which must facilitate the cooperativity in the solid state. Our observation of this SCO behavior with the FeS_2N_4 coordination set was fortuitous, but it provides motivation for further investigation of the SCO properties of Fe^{II} complexes with asymmetric coordination sets and S donor ligands.

Experimental Section

All syntheses were performed under a N_2 atmosphere using Schlenk techniques. $[Fe(OTf)_2(MeCN)_2]$ and *S*,*S*′-bis(2-pyridylmethyl)-1,2-thioethane were prepared by published procedures.[7,10] Potassium selenocyanate (Aldrich) and ascorbic acid (Merck) were used as received. Acetonitrile and water were deoxygenated by bubbling with dry N_2 gas. Solid potassium selenocyanate (72 mg, 0.50 mmol) was layered with a degassed aqueous solution of ascorbic acid (0.03 M; 1 mL) and on top of this solution, a solution of $[Fe(OTf)_2(MeCN)_2]$ (109 mg, 0.25 mmol) and *S*,*S*′-bis(2-pyridylmethyl)-1,2-thioethane (69 mg, 0.25 mmol) in degassed acetonitrile (2 mL) was layered. Crystals started to grow as the reactants diffused together. After three days, the mixture was filtered, the crystals washed with acetonitrile (2 mL) and dried by vacuum. Yield: 74 mg (55%). IR (KBr): $\tilde{\nu} = 3433$ (br), 2949 (w), 2057 (s), 1600 (m), 1567 (m), 1481 (m), 1438 (m), 1264 (m), 1156 (m), 1100 (w), 1057 (m), 1016 (m), 868 (w), 770 (m). 755 (m), 713 (m), 640 (m) cm^{-1}. Elemental analysis calcd (%) for $FeC_{16}H_{16}Se_2S_2N_4$: C 35.44, H 2.97, N 10.33. Found: C 35.78, H 2.73, N 10.22. The product consisted of a mixture of the α and γ phases with occasional traces of the β phase. If the crystals were kept in the mother liquor for a longer time (typically up to a few weeks) large dark crystals of the δ phase started to grow, resulting in the complete disappearance of α and γ phase crystals. This process was accelerated by seeding with δ phase crystals.

Received: May 30, 2012
Published online: September 28, 2012

Keywords: iron · magnetic properties · polymorphism · S ligands · spin crossover

[1] a) J. A. Real, H. Bolvin, A. Bousseksou, A. Dworkin, O. Kahn, F. Varret, J. Zarembowitch, *J. Am. Chem. Soc.* **1992**, *114*, 4650–4658; b) M. H. Klingele, B. Moubaraki, J. D. Cashion, K. S. Murray, S. Brooker, *Chem. Commun.* **2005**, 987–989; c) K. Nakano, S. Kawata, K. Yoneda, A. Fuyuhiro, T. Yagi, S. Nasu, S. Morimoto, S. Kaizaki, *Chem. Commun.* **2004**, 2892–2893; d) G. J. Halder, K. W. Chapman, S. M. Neville, B. Moubaraki, K. S. Murray, J.-F. Letard, C. J. Kepert, *J. Am. Chem. Soc.* **2008**, *130*, 17552–17562.

[2] a) M. C. Muñoz, A. B. Gaspar, A. Galet, J. A. Real, *Inorg. Chem.* **2007**, *46*, 8182–8192; b) S. M. Neville, B. A. Leita, G. J. Halder, C. J. Kepert, B. Moubaraki, J. F. Létard, K. S. Murray, *Chem. Eur. J.* **2008**, *14*, 10123–10133; c) V. Martínez, A. B. Gaspar, M. C. Muñoz, G. V. Bukin, G. Levchenko, J. A. Real, *Chem. Eur. J.* **2009**, *15*, 10960–10971.

[3] a) M. Nihei, M. Ui, M. Yokota, L. A. Han, A. Maeda, H. Kishida, H. Okamoto, H. Oshio, *Angew. Chem.* **2005**, *117*, 6642–6645; *Angew. Chem. Int. Ed.* **2005**, *44*, 6484–6487; b) M. Ruben, E. Breuning, J. M. Lehn, V. Ksenofontov, F. Renz, P. Gütlich, G. B. M. Vaughan, *Chem. Eur. J.* **2003**, *9*, 4422–4429.

[4] T. Kosone, I. Tomori, C. Kanadani, T. Saito, T. Mochida, T. Kitazawa, *Dalton Trans.* **2010**, *39*, 1719–1721.

[5] a) B. A. Leita, S. M. Neville, G. J. Halder, B. Moubaraki, C. J. Kepert, J. F. Létard, K. S. Murray, *Inorg. Chem.* **2007**, *46*, 8784–8795; b) G. S. Matouzenko, D. Luneau, G. Molnár, N. Ould-Moussa, S. Zein, S. A. Borshch, A. Bousseksou, F. Averseng, *Eur. J. Inorg. Chem.* **2006**, 2671–2682; c) R. Hinek, H. Spiering, D. Schollmeyer, P. Gütlich, A. Hauser, *Chem. Eur. J.* **1996**, *2*, 1427–1434; d) S. Bonnet, G. Molnár, J. S. Costa, M. A. Siegler, A. L. Spek, A. Bousseksou, W. T. Fu, P. Gamez, J. Reedijk, *Chem. Mater.* **2009**, *21*, 1123–1136; e) W. Hibbs, P. J. van Koningsbruggen, A. M. Arif, W. W. Shum, J. S. Miller, *Inorg. Chem.* **2003**, *42*, 5645–5653; f) J. Klingele, D. Kaase, M. H. Klingele, J. Lach, S. Demeshko, *Dalton Trans.* **2010**, *39*, 1689–1691.

[6] a) R. Pritchard, H. Lazar, S. A. Barrett, C. A. Kilner, S. Asthana, C. Carbonera, J. F. Létard, M. A. Halcrow, *Dalton Trans.* **2009**, 6656–6666; b) C. F. Sheu, S. M. Chen, S. C. Wang, G. H. Lee, Y. H. Liu, Y. Wang, *Chem. Commun.* **2009**, 7512–7514; c) M. Haryono, F. W. Heinemann, K. Petukhov, K. Gieb, P. Müller, A. Grohmann, *Eur. J. Inorg. Chem.* **2009**, 2136–2143; d) G. S. Matouzenko, E. Jeanneau, A. Y. Verat, A. Bousseksou, *Dalton Trans.* **2011**, *40*, 9608–9618; e) J. Tao, R. J. Wei, R. B. Huang, L. S. Zheng, *Chem. Soc. Rev.* **2012**, *41*, 703–737; f) C.-F. Sheu, S. Pillet, Y.-C. Lin, S.-M. Chen, I.-J. Hsu, C. Lecomte, Y. Wang, *Inorg. Chem.* **2008**, *47*, 10866–10874.

[7] a) A. Lennartson, C. J. McKenzie, *Acta Crystallogr. Sect. C* **2011**, *67*, o354–o358; b) S. E. Livingstone, J. D. Nolan, *Aust. J. Chem.* **1970**, *23*, 1553–1558.

[8] D. Chernyshov, M. Hostettler, K. W. Törnroos, H.-B. Bürgi, *Angew. Chem.* **2003**, *115*, 3955–3960; *Angew. Chem. Int. Ed.* **2003**, *42*, 3825–3830.

[9] B. Weber, W. Bauer, J. Obel, *Angew. Chem.* **2008**, *120*, 10252–10255; *Angew. Chem. Int. Ed.* **2008**, *47*, 10098–10101.

[10] K. S. Hagen, *Inorg. Chem.* **2000**, *39*, 5867–5869.

